Link Adaptation with Position/Motion Information in Vehicle-to-Vehicle Networks

Robert C. Daniels, *Member, IEEE,* and Robert W. Heath, Jr. *Fellow, IEEE*

***Abstract*—Wireless communication networks use link adaptation to select physical layer parameters that optimize the transmission strategy as a function of the wireless channel realization. In the vehicle-to-vehicle (V2V) networks considered in this letter, the short coherence time of the wireless channel makes link adaptation based on the impulse response challenging. Consequently, link adaptation in V2V wireless networks may instead exploit the large-scale characteristics of the wireless channel (i.e. path loss) since they evolve slowly and enable less frequent feedback. Large-scale channel information may be captured through channel or position/motion measurements. We show, through the definition of new large-scale coherence expressions, that channel measurements render large-scale coherence as a function of time-change while the position/motion measurements render coherence as a function of velocity-change. This letter is concluded with highway simulations of modeled and measured channels to demonstrate the advantage of position/motion information for feedback reduction in V2V link adaptation.**

***Index Terms*—**

I. Introduction

FEEDBACK enables wireless links with high data rates through link adaptation. Without link adaptation, transmitters must consider the worst case channel quality to provide reliable communication. In this letter we study link adaptation for wireless communication between two automobiles (also called *vehicle-to-vehicle* (V2V) wireless communication). Because the transmitter and receiver are typically moving at high speeeds in potentially opposite directions, multipath changes very rapidly, especially at higher frequencies. V2V communication is also intermittent since links appear and disappear very quickly. Therefore, it is critical that the maximum amount of information is transferred when a link is active. Clearly, link adaptation is important for future V2V networks that will carry important driver safety and traffic information [1]. It may not be feasible, however, to provide complete channel feedback for link adaptation in V2V wireless links. Channel measurements of V2V links have shown that the coherence time is sometimes less than 1 msec due to the high mobility of vehicles in highway scenarios [1], [2]. The protocol delay of feedback between vehicles may exceed this coherence time. For example, the immediate feedback exchange in IEEE 802.11n provides at best $\approx 0.1 - 3.0$ msec of feedback delay [3]. Moreover, low-latency, high-rate feedback protocols yield large overhead, which reduces link adaptation utility.

To enable link adaptation for wireless communications over channels with a short coherence time, several have proposed protocols that exploit large-scale channel information, i.e., path loss [4]–[6]. For link adaptation with path loss, the receiver may feed back one of two measurements: **1**) received signal strength **2**) position/motion information [7]. Position/motion information is made available by GPS or similar localization technologies which have become pervasive in vehicular environments [8], [9]. For **1**) the transmitter must complete a windowed average of received signal strength to estimate path loss. In **2**) the transmitter first predicts the communication distance based on the current transmitter position and the expected receiver position given position/motion feedback. The transmitter computes path loss after distance prediction through, for example, the log-distance model or inverse wireless fingerprinting [10], [11].

This letter studies the preference of feeding back **1**) or **2**) to enable link adaptation in V2V links. We propose a new metric to measure the consistency of path loss: *large-scale coherence*. We use this metric to propose expressions of *large-scale coherence time* and *large-scale coherence velocity* in log-distance path loss models. Large-scale coherence time quantifies the freshness of the path loss estimate at the transmitter through feedback with **1**) while large-scale coherence velocity quantifies the freshness of the derived path loss estimate at the transmitter through feedback with **2**). Intuitively, assuming that vehicle position trajectory between feedback periods is completely characterized by 1st and 2nd order information (vehicle velocity and acceleration), with **1**) we cannot infer the location of vehicles between feedback periods so we cannot infer the variation of path loss between feedback periods. To determine the interval of feedback, we simply find the time that the channel becomes large-scale incoherent as a function of vehicle position, velocity, and acceleration. In **2**), without acceleration, we can indefinitely determine path loss with one feedback exchange. Hence, large-scale channel incoherence is fundamentally tied to the coherence of vehicle velocity, or acceleration. Using these new expressions we will show that, through simulation studies of V2V highway communications, position/motion feedback requires less overhead than link adaptation with received power measurements.

Assumptions: This work assumes that each path loss or position/motion feedback exchange requires the same time allocation on the network. Therefore, the rate of feedback will determine whether link adaptation with **1**) or **2**) incurs more

Manuscript received January 14, 2011; revised August 1, 2011; accepted November 7, 2011. The associate editor coordinating the review of this letter and approving it for publication was Dr. G. Song.

The authors are with the Wireless Networking & Communications Group in Dept. of Elect. & Comp. Eng. at the University of Texas at Austin, 1 University Station C0803, Austin, TX 78712-0240, **fax**: +1 512.417.6512 (e-mail: robert.daniels@utexas.edu, rheath@ece.utexas.edu). R. C. Daniels is also with Kuma Signals, LLC, Austin, TX.

Work funded by Army Research Laboratory Contract W911F-08-1-0438.
Digital Object Identifier 10.1109/TWC.2011.110086.

overhead. While our simulations include accurate path loss measurements, our proposed coherence expressions assume simplistic path loss models. These simple models help us to develop intuition in the tradeoff between link adaptation with position and motion information. Our results also assume that path loss and position information can be resolved exactly, which will not be the case for either in practice. Relaxation of these assumptions will be treated as future work.

II. Large-Scale Channel Coherence

Consider single-antenna, frequency-flat channels where realization $h(t) \in \mathbb{C}$ is decomposed into small- and large-scale effects such that $h(t) = \sqrt{\alpha(t)}\beta(t)$ where $t \in [0, \infty)$ is the relative time (arbitrarily starting at 0), $\alpha(t) \in (0, 1]$ is the time-varying large-scale channel component due to path loss, and $\beta(t)$ is due to small-scale effects resulting from time-varying multipath (statistically $\beta(t)$ could represent Rayleigh fading, for example).

A. Channel Coherence Definitions

The minimum feedback rate for link adaptation is typically determined by the coherence time of the channel [12]. Calculation of channel coherence through the correlation coefficient of the impulse response is not relevant here, however, since we consider link adaptation based on path loss.

Definition 1. *Using $t_1 \geq 0$ as our initial time reference and $t_2 > t_1$, we propose*

$$\frac{\alpha(t_2)}{\alpha(t_1)} < \eta \textbf{ or } \frac{\alpha(t_2)}{\alpha(t_1)} > \frac{1}{\eta} \tag{1}$$

implies that $\alpha(t_2)$ is **large-scale incoherent** *at time t_2 with respect to $\alpha(t_1)$ for $\eta \in (0, 1]$.*

Our definition of large-scale channel coherence was inspired by observing adaptive modulation and coding (AMC). Typically, the different AMC strategies are separated (approximately) by the same difference in average SNR on a logarithmic scale. For example, using the AMC system in [13], the average SNR gap is around 3 dB $\Rightarrow 10\log_{10}(\eta) \approx 3 \Leftrightarrow \eta \approx 0.5$. Therefore our definition allows us to relate large-scale channel incoherence with a change in transmission strategy. Moreover, (1) allows us to fairly and accurately characterize large-scale channel coherence using both path loss measurements and position/motion measurements in the next two subsections.

B. Vehicle-to-Vehicle Large-Scale Channel Coherence

Consider a V2V wireless link between two vehicles which both lie in 3-dimensional Euclidean space to model a general propagation environment. The position and motion (velocity) of the first vehicle as a function of time are represented as $\mathbf{p}(t) = [p_1(t), p_2(t), p_3(t)]^T$ and $\mathbf{m}(t) = [m_1(t), m_2(t), m_3(t)]^T$, respectively, where each are defined in $\mathbb{R}^3$. Similarly, the position and motion of the second vehicle are defined by $\mathbf{q}(t)$ and $\mathbf{n}(t)$. We assume path loss may be defined in terms of position and time, i.e. $\alpha(t)$ is deterministic if $\mathbf{p}(t)$ and $\mathbf{q}(t)$ are known.

Consider that position and motion information are measured and known at time t_1. For $t_2 > t_1$, assuming that higher order statistics of position (acceleration and above) vary too quickly to measure accurately, we estimate/predict the position information at t_2 with only velocity, i.e. $\hat{\mathbf{p}}(t_1, t_2) \triangleq \mathbf{p}(t_1) + (t_2 - t_1)\mathbf{m}(t_1)$ ($\hat{\mathbf{q}}(t_1, t_2)$ is defined similarly). We also define the predicted distance through velocity information, $\hat{\mathbf{d}}(t_1, t_2) \triangleq \|\hat{\mathbf{p}}(t_1, t_2) - \hat{\mathbf{q}}(t_1, t_2)\|_2$. The accuracy of the predicted path loss at t_2 through $\hat{\mathbf{d}}(t_1, t_2)$ depends on variation of $\mathbf{m}(t)$ and $\mathbf{n}(t)$ over $t \in [t_1, t_2]$. Thus, we have two measures of large-scale coherence: with path loss measurements (*large-scale coherence time*) and with position/motion measurements (*large-scale coherence velocity*).

To bound the change in $\mathbf{m}(t)$ and $\mathbf{n}(t)$ over the interval $t \in [t_1, t_2]$ and determine large-scale coherence in terms of velocity change, we assume linear acceleration for both vehicles. We define $\boldsymbol{\delta} \triangleq ((\mathbf{m}(t_2) - \mathbf{n}(t_2)) - (\mathbf{m}(t_1) - \mathbf{n}(t_1)))/(t_2 - t_1)$ as the relative acceleration between the first and second vehicle. Assuming $\boldsymbol{\delta}$ completely characterizes the change in velocity over $[t_1, t_2]$, the inter-vehicle distance at t_2 is defined $\mathbf{d}(t_1, t_2, \boldsymbol{\delta}) \triangleq \|\mathbf{p}(t_1) - \mathbf{q}(t_1) + (t_2 - t_1)\left(\frac{\boldsymbol{\delta}}{2}(t_2 - t_1) + \mathbf{m}(t_1) - \mathbf{n}(t_1)\right)\|_2$. The large-scale coherence time of the channel can now be defined in terms of the relative acceleration

$$\tau_c(t_1, \boldsymbol{\delta}, \eta) \triangleq \min_{t_2 \in (t_1, \infty)} \{t_2 - t_1 : \alpha(t_1)/\alpha(t_1, t_2, \boldsymbol{\delta}) = \mu(\eta)\} \tag{2}$$

where $\alpha(t_1, t_2, \boldsymbol{\delta})$ is the path loss mapped from $\mathbf{d}(t_1, t_2, \boldsymbol{\delta})$ and the term $\mu(\eta) \triangleq \eta$ if $\alpha(t_1, t_2, \boldsymbol{\delta}) > \alpha(t_1)$ and $\mu(\eta) \triangleq 1/\eta$ otherwise. Similarly, the large-scale coherence velocity region of the channel can be defined in terms of the interval $[t_1, t_2]$,

$$\nu_c(t_1, t_2, \eta) \triangleq \{\boldsymbol{\delta} : \hat{\alpha}(t_1, t_2)/\alpha(t_1, t_2, \boldsymbol{\delta}) = \mu(\eta)\} \subset \mathbb{R}^3 \tag{3}$$

given $\hat{\alpha}(t_1, t_2)$ is the path loss mapped from $\hat{\mathbf{d}}(t_1, t_2)$. Here, $\mu(\eta) \triangleq \eta$ if $\hat{\alpha}(t_1, t_2) < \alpha(t_1, t_2, \boldsymbol{\delta})$ and $\mu(\eta) \triangleq 1/\eta$ otherwise. Therefore, large-scale coherence velocity is the set of relative acceleration thresholds that, when met, cause the predicted path loss at t_2 through position/motion information, $\hat{\alpha}(t_1, t_2)$, to become large-scale incoherent.

C. V2V Large-Scale Coherence in Log-Distance Model

For a deeper insight into the definition of large-scale coherence time and large-scale coherence velocity in V2V networks, let us consider the log-distance path loss model with path loss exponent n and path loss reference measurement value γ_0 at reference distance d_0. [10]. With this model $\alpha(t) = \gamma_0 (d_0/d(t))^n$ where $d(t) \triangleq \|\mathbf{p}(t) - \mathbf{q}(t)\|_2$ is the distance between the first and second vehicle. By redefining the numerator in terms of the velocities and acceleration, the path loss measurement at time t_1 results in large-scale channel incoherence at t_2 if

$$\mu(\eta) = (d(t_1, t_2, \boldsymbol{\delta})/d(t_1))^n \tag{4}$$

$$\Rightarrow \; b_4\Delta_t^4 + b_3\Delta_t^3 + b_2\Delta_t^2 + b_1\Delta_t + b_0 = 0 \tag{5}$$

for $\Delta_t \triangleq (t_2 - t_1)$, $b_0 \triangleq \left(1 - \mu(\eta)^{2/n}\right) d(t_1)^2$, $b_1 \triangleq \sum_{k=1}^{3} 2(m_k(t_1) - n_k(t_1))(p_k(t_1) - q_k(t_1))$, $b_2 \triangleq \sum_{k=1}^{3} \delta_k(p_k(t_1)$

Fig. 1. Illustration of network topology. Two vehicles approaching each other where the x-axis represents the position of each vehicle. At t_1 node 1 accelerates at δ m/s^2 until t_2 when the vehicle stops acceleration.

$-q_k(t_1)) + (m_k(t_1) - n_k(t_1))^2$, $b_3 \triangleq \sum_{k=1}^{3} \delta_k(m_k(t_1) - n_k(t_1))$, and $b_4 \triangleq \sum_{k=1}^{3} \delta_k^2/4$. The large-scale coherence time is the minimum non-negative root of this quartic polynomial. Similarly, large-scale incoherence through position/motion information occurs at t_2 when

$$\mu(\eta) = \left(d(t_1,t_2,\boldsymbol{\delta})/\hat{d}(t_1,t_2)\right)^n \quad (6)$$

$$\Leftrightarrow \quad \|\boldsymbol{\delta}+\mathbf{a}\|_2^2 = \mu(\eta)^{\frac{2}{n}}\|\mathbf{a}\|_2^2 \quad (7)$$

$$\Rightarrow \quad \|\boldsymbol{\delta}\|_2^2 \geq (\mu(\eta)^{\frac{2}{n}}-1)\|\mathbf{a}\|_2^2 \quad (8)$$

by Cauchy-Schwarz where $\mathbf{a} \triangleq \frac{2}{\Delta_t^2}(\mathbf{p}(t_1) - \mathbf{q}(t_1) + \Delta_t(\mathbf{m}(t_1) - \mathbf{n}(t_1)))$. We can also define an upper bound on each relative acceleration component by setting the other components equal to zero and solving the quadratic equation in (8). Thus, for $\mathbf{a} = [a_1, a_2, a_3]^T$, the inequality

$$|\delta_k| \leq \max\left\{\left|a_k(1+\mu(\eta)^{2/n})\right|, \left|a_k(1-\mu(\eta)^{2/n})\right|\right\} \quad (9)$$

provides an upper bound on each component of the coherence velocity. Hence, in the general 3-dimensional propagation scenario we cannot complete a simple large-scale coherence velocity expression due to the 2 degrees of freedom available in the acceleration components. We can, however, place lower and upper bounds on the acceleration values. Notice that as $n \to \infty$ (path loss exponent increases indefinitely), the upper bound limit per dimension is $2|a_k|$. It can also be shown in (5) that as $n \to \infty$, $b_0 \to 0 \Rightarrow \tau_c(t_1, \boldsymbol{\delta}, \eta) \to 0$. Hence, the larger the path loss exponent, the more attractive position information becomes for estimating path loss. In 1-dimensional spaces, such as the system in the sequel, the expressions for large-scale coherence time *and* large-scale coherence velocity simplify dramatically.

III. Highway Study of V2V Link Adaptation

To demonstrate the practical significance of the large-scale coherence expressions in Section II, we consider the highway V2V network topology. We show simplified large-scale coherence expressions due to the position dimensionality reduction. Feedback rate tradeoffs are simulated for practical operating conditions to demonstrate that position/motion information availability often results in less feedback exchanges.

A. Large-Scale Coherence Expressions in 1-D

We now proceed with the computation of large-scale coherence time for the V2V network topology in Fig. 1. We consider the scenario where two vehicles are traveling on a line and the path loss between them is modeled by the Friis free space propagation formula ($n = 2$, $d_0 = 1$, $\gamma_0 = (\lambda/4\pi)$ with operating wavelength λ meters in the log-distance path loss model). We only consider a single accelerating vehicle (node 1 acceleration $= \delta$, node 2 acceleration $= 0$), since relative acceleration determines large-scale coherence velocity. For 1 dimension, (4) simplifies to

$$\sqrt{\mu(\eta)} = \frac{\left|q(t_1) - p(t_1) + (n(t_1) - m(t_1))\,\Delta_t - \frac{\delta}{2}\Delta_t^2\right|}{|q(t_1) - p(t_1)|} \quad (10)$$

$$\Rightarrow \tau_c(t_1,\delta,\eta) = \frac{m(t_1)-n(t_1)}{\delta} \pm \frac{\sqrt{(m(t_1)-n(t_1))^2 - 2\delta\left(\kappa\sqrt{\mu(\eta)}-1\right)d(t_1)}}{\delta} \quad (11)$$

where $\kappa = 1$ if the sign inside the absolute value of the numerator and denominator in (10) match, otherwise $\kappa = -1$. If the signs do not match, this means that node 1 and node 2 cross paths, i.e. the crossover point is in the interval (t_1, t_2) such that their direction relative to each other has changed. We can similarly simplify large-scale coherence velocity. Equation (6) simplifies to

$$\sqrt{\mu(\eta)} = \frac{\left|q(t_1) - p(t_1) + (n(t_1) - m(t_1))\,\Delta_t - \frac{\delta}{2}\Delta_t^2\right|}{|q(t_1) - p(t_1) + (n(t_1) - m(t_1))\,\Delta_t|} \quad (12)$$

$$\Rightarrow \nu_c(t_1,t_2,\eta) = \frac{2\left(\kappa\sqrt{\mu(\eta)}-1\right)(q(t_1) - p(t_1) + \Delta_t\,(n(t_1) - m(t_1)))}{\Delta_t^2} \quad (13)$$

where κ is defined the same manner as before. We now have simple expressions that characterize the large-scale coherence time and the large-scale coherence velocity in 1-dimensional space.

B. Large-Scale Coherence Simulations in 1-D

The 1-dimensional V2V link with free space path loss simplifies a very interesting practical scenario: highway communication as shown in Fig. 1. Reflective paths (for example ground reflections) are assumed to contribute primarily to multipath and not path loss [14]. Since we are adapting based on path loss they are not considered here. Moreover, adding complexity to the channel model will lead to tractability issues, limiting the resulting system design intuition. We use (11) and (13) to define the large-scale coherence time and large-scale coherence velocity. The large-scale coherence boundary, where the large-scale coherence time equals the large-scale coherence velocity, can be solved by evaluating the quadratic equations produced by $\nu_c(t_1, \tau_c(t_1,\delta,\eta)+t_1, \eta)$ and $\tau_c(t_1, \nu_c(t_1,t_2,\eta),\eta)$ in terms of δ, t_1 and $t_1, t_2 - t_1$, respectively.

Examine the following highway scenario with maximum link distance of 3 km in free space: $m(t) = 25$ m/s (≈ 55 mph) for $t \in [0, t_1]$, $n(t) = -30$ m/s (≈ 65 mph) for $t \in [0, \infty)$, $p(0) = 0$, $q(0) = 3000$, and $\eta = 0.5$. Figs. 2 and 3 show the large-scale coherence time and large-scale coherence velocity contours, respectively. Fig. 2 demonstrates that large-scale coherence time is much larger than traditional coherence time for the highway scenario. Figs. 2 and 3 lend considerable insight into the tradeoff between the feedback of path loss information and the feedback of position/motion information. For any realization of t_1 and δ we can find whether feedback

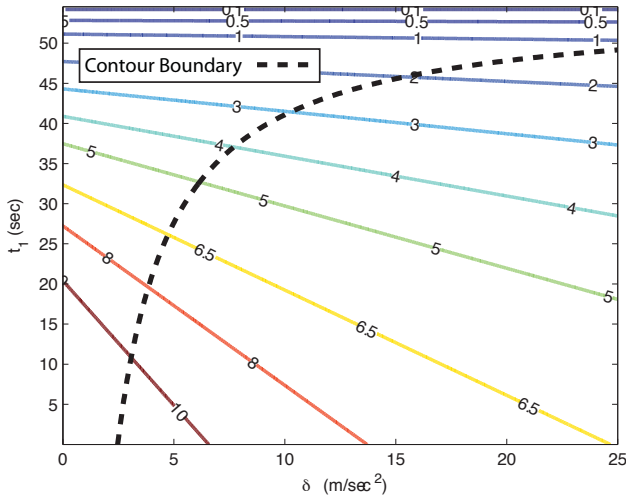

(a) Contour plot of τ_c

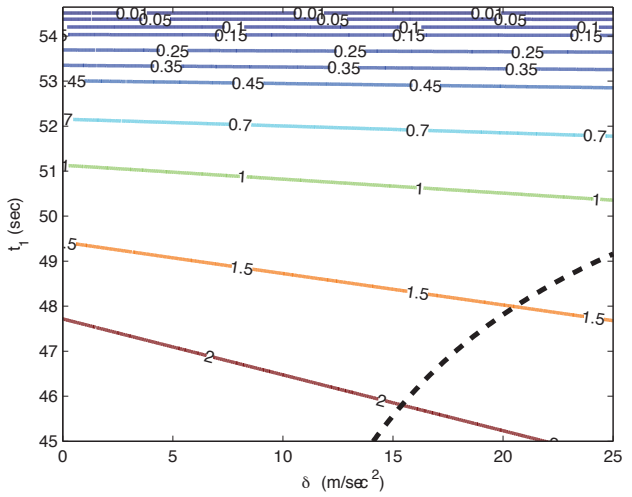

(b) Close up view of τ_c contour plot

Fig. 2. The numbers on each line in Fig. 2(a) and Fig. 2(b) represent the values for each large-scale coherence time contour in seconds. The time reference t_1 is only considered in the interval $[0, 54.545]$ since $t_1 = 54.545$ is the crossover time under no acceleration. We can see that near the crossover point the coherence time decreases rapidly. This is a consequence of free space path loss which is inversely proportional to vehicular distance squared. The dashed line represents the contour boundary. The region to the right of the contour boundary represents scenarios where path loss information results in less feedback overhead whereas the region to the left of the contour boundary shows where position/motion information is preferred.

of position/motion information is advised by observing the black dotted line (contour boundary). In Fig. 2, realizations of δ, t_1 to the left of the contour boundary show acceleration values (and the associated time reference t_1) that result in less feedback overhead with position/motion information than path loss information. Similarly, in Fig. 3, contour points to the right of the black dotted line represents node 1 acceleration that results in link adaptation with less feedback overhead for position/motion information.

Practically speaking, in typical driving scenarios, the maximum acceleration is somewhere between $3 - 5$ m/s^2. High-performance vehicles achieve a maximum of around 8 m/s^2 in racing conditions. Consequently, for most conceivable V2V network scenarios, the overhead incurred for feedback of position information to accomplish link adaptation in the

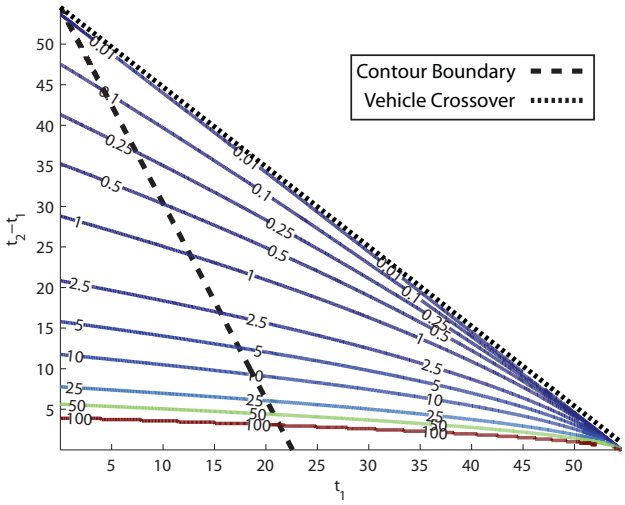

Fig. 3. The numbers on each line represent the values for each large-scale coherence velocity contour in m/s^2. The vehicle crossover point for each realization of t_1, t_2 is shown with the fine dotted line. For time reference t_1, the maximize acceleration tolerable to maintain large-scale channel coherence at t_2 is found on the contour that intersects $(t_1, t_2 - t_1)$. The contour boundary shows the intersection of $\boldsymbol{\delta}$ and $\nu_c(t_1, t_2, \eta)$ where $\boldsymbol{\delta}$ is selected such that $\tau_c(t_1, \boldsymbol{\delta}, \eta) = t_2 - t_1$. Hence, values to the right of the contour boundary show scenarios where position/motion information results in less feedback overhead than path loss information.

highway scenario is favorable when compared to the overhead incurred for the feedback of path loss information. Most importantly, near the crossover point, where the path loss changes very rapidly, position/motion information is preferred for all realizable acceleration scenarios.

C. Simulation with Highway Path Loss Measurements

The 1-D coherence models and simulations are important for insight into channel dynamics in the context of position and motion information, however, they are insufficient for creating link adaptation algorithms in practice due to the presence of reflected paths, shadows (path blockages), and atmospheric absorption. For final validation of position and motion information, link adaptation simulations are completed with highway path loss measurements at 5.2 GHz as reported in [2]. These measurements report path loss captured over 10 seconds on a highway (in Sweden) between two vehicles traveling in opposite directions at a relative speed of 180 km/hr (includes vehicle crossover), as recreated in Figure 4. We model link adaptation in IEEE 802.11p by assigning each transmission one of the eight modulation and coding schemes that provide 6-54 Mbps in 20 MHz spectrum allocations. We use the sensitivity requirements defined in the standard (Table 17-13 of [3]) to determine if communication is successful (which means that the transmitter will select the highest rate that meets the sensitivity requirements). We will assume that one node is designated as the transmitter and the other as the receiver with path loss given by [2].

The baseline link adaptation algorithm with *aperiodic feedback* does not have position or motion information so it must send back channel information whenever the channel becomes incoherent with respect to the last feedback exchange. Aperiodic feedback is optimistic since traffic may be bursty, resulting in stale path loss information at the receiver. This motivates

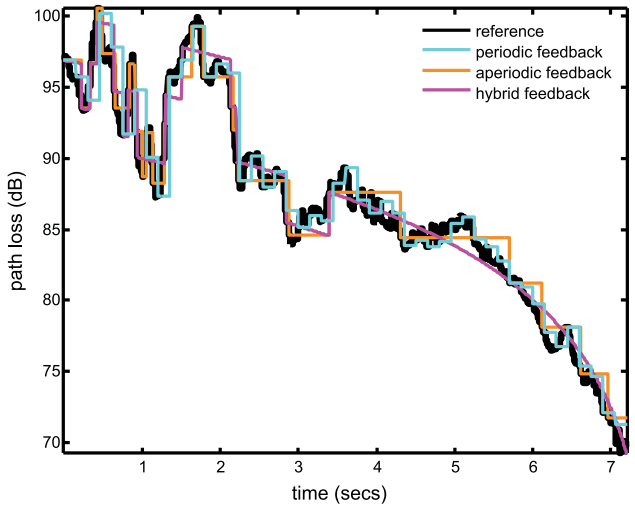

Fig. 4. Path loss (reference curve) reproduced from [2] for V2V highway channel measurements at 5.2 GHz. Path loss depicted until vehicle crossover for opposing vehicles traveling at a relative velocity of 180 km/hr. The various forms of feedback allow the transmitter to maintain estimates of the path loss. The transmitter-predicted path loss estimates shown here through various feedback strategies assume $\eta = 0.5$.

Feedback Strategy	$\eta = 0.794$	$\eta = 0.631$	$\eta = 0.500$
Aperiodic	$71/35.7$	$37/33.2$	$24/31.1$
Periodic	$480/35.8$	$144/33.3$	$120/31.1$
Hybrid	$73/36.0$	$28/33.2$	$14/31.7$

TABLE I
x/y - x FEEDBACK EXCHANGES REQUIRED BY FEEDBACK STRATEGY, RESULTING IN AVERAGE RATE OF y MBPS IN IEEE 802.11P LINK ADAPTATION SIMULATION WITH MEASURED PATH LOSS ON A HIGHWAY IN SWEDEN AT 5.2 GHZ (FIRST 7.2 SECONDS SIMULATED, IMMEDIATELY BEFORE VEHICLE CROSSOVER) [2]. RESULTS ARE SHOWN IN TERMS OF THE THE LARGE-SCALE COHERENCE METRIC $(1, 2, 3$ DB$)$ WITH THE CONSTRAINT OF ZERO EMPIRICAL OUTAGE.

link adaptation with *periodic feedback* which is pessimistic since it sends back path loss information at regular intervals regardless of how much path loss estimates have changed. To incorporate position and motion information, we cannot use straightforward feedback due to model and measurement inconsistencies. Our solution is a *hybrid feedback* protocol which sends back position, motion, *and* path loss information. The path loss information is required to re-initialize the log-distance path loss model for each feedback exchange. Feedback exchanges only occur during large-scale incoherency. To prevent stale path loss exchanges (as in aperiodic feedback) we piggyback transmitter path loss information with the first data packet after each feedback exchange.

Table I shows that, even in the presence of log-distance model inaccuracy, position and motion information can be leveraged to substantially reduce feedback in V2V large-scale link adaptation without compromising performance. The transmit power is set at 20 dBm to ensure that all modes (6-54 Mbps in 20 MHz channels) are required for optimal rate adaptation. To provide zero outage we add an η penalty factor to the path loss estimate at the transmitter, which is used to select the mode. Strategically decreasing this penalty may provide controlled nonzero outage for aperiodic and hybrid feedback strategies. Results show that position and motion information can substantially reduce feedback without compromising data rate (except when η close to 1 due to inaccuracy of log-distance path loss models in practice). Note that acceleration information is not needed to complete this study nor is previous knowledge of the ideal path loss coefficient ($n = 2$ was used for results in Table I and empirically we observed that varying this parameter between 1 and 3 did not significantly impact performance).

IV. CONCLUSION

In this letter we considered the use of position/motion information in V2V networks. To this end we defined coherence as a function of time and velocity change in path loss models. Simulations demonstrate the value of position/motion information to reduce feedback overhead.

ACKNOWLEDGEMENTS

The authors would like to thank Steven W. Peters for valuable discussions that led to this work as well as the anonymous reviewers who encouraged enhancement of the simulation results.

REFERENCES

[1] D. Matolak, "Channel modeling for vehicle-to-vehicle communications," *IEEE Commun. Mag.*, vol. 46, no. 5, pp. 76–83, May 2008.
[2] A. Paier *et al.*, "Description of vehicle-to-vehicle and vehicle-to-infrastructure radio channel measurements at 5.2 GHz," in *COST 2100, 6th Management Committee Meeting*, Lille, France, Oct. 2008.
[3] "IEEE standard for information technology - part 11: Wireless LAN medium access control and physical layer specifications," *IEEE Std 802.11-2007*, 12 2007.
[4] J. Gozalvez and J. Dunlop, "On the dynamics of link adaptation updating periods for packet switched systems," *Wireless Personal Commun.*, vol. 23, no. 1, pp. 137–145, 2002.
[5] S. J. Lee, "Trade-off between frequency diversity gain and frequency-selective scheduling gain in OFDMA systems with spatial diversity," *IEEE Commun. Lett.*, vol. 11, no. 6, pp. 507–509, June 2007.
[6] H. Touheed, A. Quddus, and R. Tafazolli, "An improved link adaptation scheme for high speed downlink packet access," *IEEE Veh. Technol. Conf.*, pp. 2051–2055, May 2008.
[7] H. Celebi and H. Arslan, "Utilization of location information in cognitive wireless networks," *Wireless Commun., IEEE*, vol. 14, no. 4, pp. 6–13, Aug. 2007.
[8] J. Hernandez and C.-Y. Kuo, "Steering control of automated vehicles using absolute positioning GPS and magnetic markers," *IEEE Trans. Veh. Technol.*, vol. 52, no. 1, pp. 150–161, Jan. 2003.
[9] Z. Li, L. Sung, and E. C. Ifeachor, "Range-based relative velocity estimations for networked mobile devices," *IEEE Trans. Veh. Technol. (to appear)*, 2009.
[10] T. S. Rappaport, *Wireless Communications: Principles and Practice (2nd Edition)*. Prentice Hall PTR, Dec. 2001.
[11] B. Li, Y. Wang, H. Lee, A. Dempster, and C. Rizos, "Method for yielding a database of location fingerprints in WLAN," *IEE Proc.-Commun.*, vol. 152, no. 5, pp. 580–586, Oct. 2005.
[12] J. Camp and E. Knightly, "Modulation rate adaptation in urban and vehicular environments: Cross-layer implementation and experimental evaluation," in *Proc. 14th ACM Mobicom*, 2008, pp. 315–326.
[13] S. Choudhury and J. Gibson, "Payload length and rate adaptation for multimedia communications in wireless LANs," *IEEE J. Sel. Areas Commun.*, vol. 25, no. 4, pp. 796–807, May 2007.
[14] D. Matolak, I. Sen, W. Xiong, and N. Yaskoff, "5 GHz wireless channel characterization for vehicle to vehicle communications," in *IEEE Military Commun. Conf.*, vol. 5, Oct. 2005, pp. 3016–3022.